

## A ROLE OF TEXTURE IN CONTROLLING OXIDATION AND HYDROGEN INGRESS IN ZR-NB PRESSURE TUBES

HUALONG LI<sup>1,2</sup>, JIANLONG LIN<sup>1</sup> AND JERZY SZPUNAR<sup>1</sup>

<sup>1</sup>Department of Metallurgical Eng., McGill University, Montreal, H3A 2B2

<sup>2</sup>ResMat Corp., Suite 320, 3637 University, Montreal, H3A 2B3

### ABSTRACT

A nano-scale microstructural computer model for predicting ZrO<sub>2</sub> structure and texture development during oxidation of Zr-Nb alloy has been proposed. The model assumes that the main driving force for texture formation in oxide and growth of the oxide grains is the compression stress parallel to the oxide surface. The orientation of substrate grains also plays an important role. The oxide texture, microstructure, grain boundary character distribution and the stress development can be simulated. The substrate texture, microstructure, phase composition are the major factors determining the oxide structure. This structure controls the oxygen and hydrogen transport through oxide layer; therefore the model that predicts the oxide structure allows the simulation of the corrosion behaviour and hydrogen ingress through the oxide. The proposed model has been used to predict the Zr oxidation kinetics in air for different textures of the substrate. The result of simulation agrees with character of changes observed in oxidation experiments. Eventually, this model will be able to simulate the hydrogen ingress process and to predict hydride formation and cracking of the pressure tube. The comparison between the simulation and experimental results will be presented.

### INTRODUCTION

Zr-2.5% Nb alloy pressure tubes are used in the core of CANDU nuclear power reactors. During the operation of the reactor, oxidation takes place at both the interior and exterior surfaces of the pressure tube. The oxide film formed on the pressure tube surface serves as a protective barrier against hydrogen ingress. Therefore, ability to predict and control the oxide structure is important to ensure safe operation of the reactor.

Our earlier research work<sup>2-14</sup> has been focused on understanding the oxidation mechanism and oxide texture and microstructure development. Recently, efforts have been made to develop software that will eventually allow to predict the oxide structure development and to optimize the parameters that control the oxide structure.

### THEORETICAL BACKGROUND

The Zr alloy oxidation process is controlled by inward diffusion of oxygen<sup>16</sup>, mainly along oxide grain boundaries. Thus, the oxide grain boundary density and grain boundary character distribution are considered important factors in controlling oxidation. The oxygen transport along

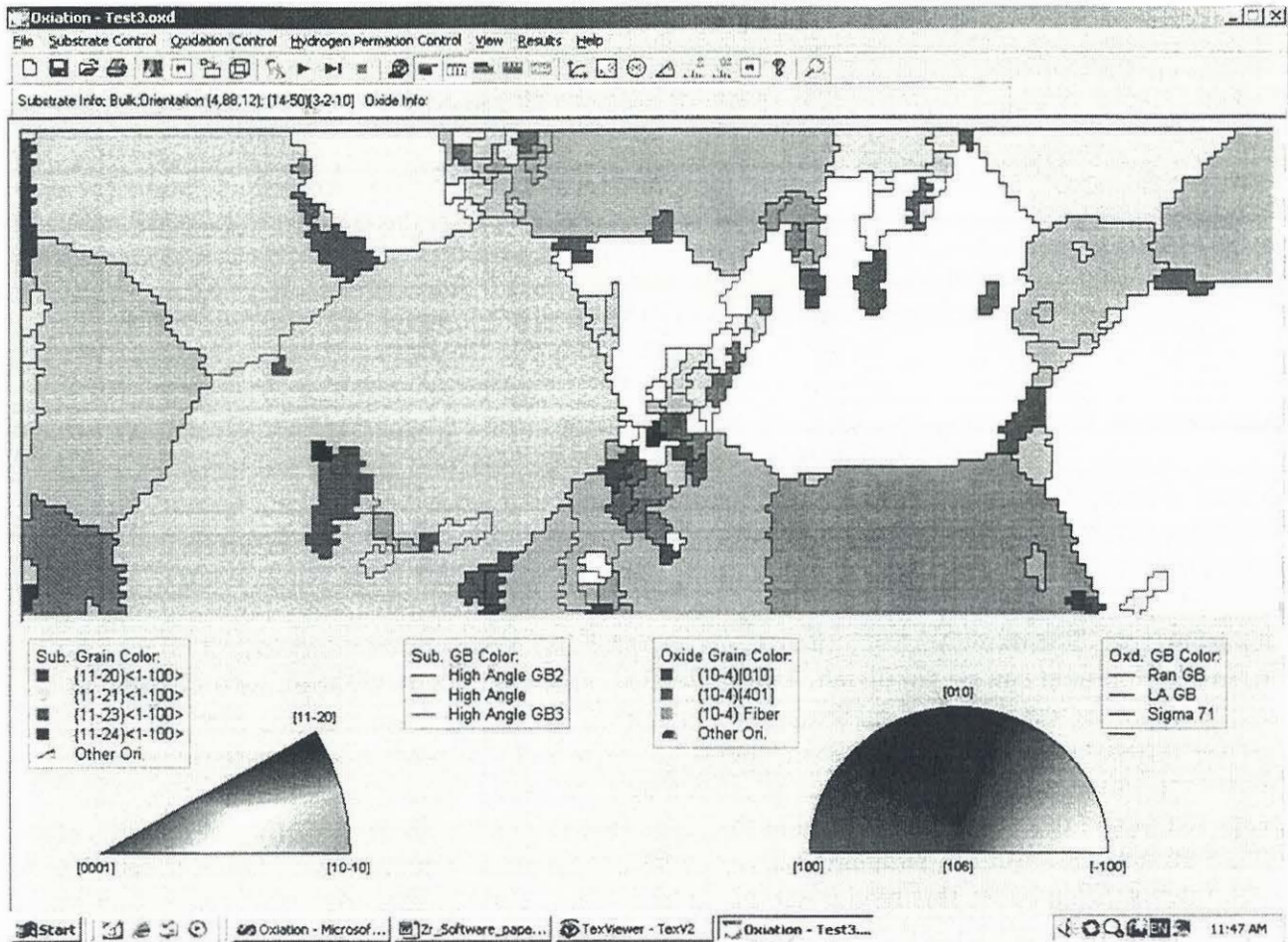


Fig. 1 The main user interface of the software

the oxide grain boundaries depends on the oxide grain size and oxide grain boundary character distribution and is determined by oxide texture. In agreement with our research results and results obtained by other researchers<sup>2-14, 15, 17-25</sup>, we made the following assumptions:

- Zr oxidation process can be divided into two stages: selective nucleation stage and selective grain growth stage.
- In nucleation stage, the oxide nucleation takes place on substrate surface and in  $\alpha$ -Zr grain boundaries and  $\beta$ -Zr locations. The oxide orientation is determined by lattice matching when there is a  $\alpha$ -Zr grain near the nucleation site. Oxide has random orientation when nucleation takes place in  $\beta$ -Zr. Nucleation does not take place inside  $\alpha$ -Zr grains.
- In oxide grain growth stage, the grains with (10-4) crystallographic plane parallel to the sample surface grow fast, in order to reduce the elastic energy caused by the compression stress in the oxide film.

## HOW THE MODEL WORKS

Figure 1 shows the main user interface of the software. The starting point of the simulation is to define the microstructure of the Zr substrate. The source of information on Zr substrate can be one of the followings experimental techniques:

1. OIM (Orientation Imaging Microscopy) measurement. OIM data is the best input to the software because it contains grain size, grain shape, grain orientation, grain boundary character, and phase composition of the substrate. The microstructure shown in Fig. 1 is an OIM image of pure Zr substrate. We choose pure Zr substrate for demonstration purpose because it has larger grain size compared with Zr-Nb and other Zr alloys.
2. SEM measurement. SEM images can also be used as an input to the software. The grain orientation and phase composition can be obtained from diffraction measurements.
3. Computer generated microstructure. In this microstructure the grain orientation and phase composition can be determined from diffraction experiments

The oxidation process that is described by the transformation of the oxide texture, microstructure and grain boundary network is governed by the mechanism described in the previous section. As the oxide grows, the oxygen and hydrogen diffusion processes take place simultaneously. The diffusion processes are simulated based on Random-Walk theory; the simulation details and mathematical treatment can be found in reference [1, 2]. Basically, the jumping frequency of atom is determined by the local diffusivity. Atoms in the locations with high diffusivities jump fast and vice versa.

Generally, bulk, twin boundaries, and low angle grain boundaries have less free volume than high angle grain boundaries; therefore, they usually have higher diffusion activation energies and represent slow diffusion path. For example, Fig. 2 shows the diffusion activation energies as a function of  $\langle 100 \rangle$  tilt angle in cubic  $\text{ZrO}_2$  system calculated using molecular dynamic method<sup>4</sup>. One can see that low angle grain boundaries (tilt angle less than 20 or higher than 70) have higher diffusion activation energies, which indicate slower diffusion along these boundaries.

The diffusion coefficients of different types of monoclinic  $\text{ZrO}_2$  grain boundaries are not reported in literature. In order to perform the simulation, we made the following assumptions. We roughly classify the oxide grain boundaries into three types: special grain boundaries ( $\Sigma 3$  and

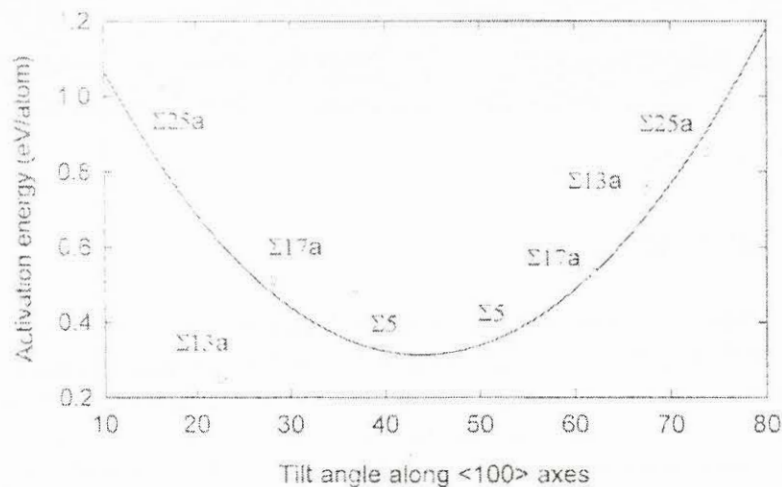


Fig. 2 Calculated diffusion activation energies of  $\langle 100 \rangle$  axes CSL grain boundaries in cubic  $\text{ZrO}_2$  system

71), low angle ( $< 15^\circ$ ) grain boundaries and high angle grain boundaries.  $\Sigma 3$  and 71 boundaries have almost zero free volume<sup>8</sup>. Therefore, when oxygen atoms pass through these grain boundaries, they must overcome the same energy barrier as when they pass through the bulk. As a result, the diffusivities along these grain boundaries are treated the same as that of bulk. In  $ZrO_2$  oxide, the oxygen diffusion along grain boundaries is believed to be predominant<sup>16, 17, 28</sup>. The contribution of bulk diffusion to the oxidation process is insignificant and is neglected in the simulation. For low angle grain boundaries, the diffusion coefficient is roughly estimated as the half of that of high angle grain boundaries. In other words, the diffusion coefficients of three types of grain boundaries used in the simulation are 0, 0.5, and 1 respectively.

Fig. 3 and 4 show two examples of the simulation. In figure 3, one can see the oxide nucleates in the region where the original  $\alpha$ -Zr grain boundaries and  $\beta$ -Zr regions are located. Due to frequent nucleation events, the oxide grains in these areas are small. The oxide grains grow continually if they are inside the  $\alpha$ -Zr grains and thus are large. Figure 4 shows that significant amount of special grain boundaries ( $\Sigma 3$  and 71) can be formed due to the lattice matching. Along those special grain boundaries, the oxygen diffusion rate is lower than along random oxide grain boundaries.

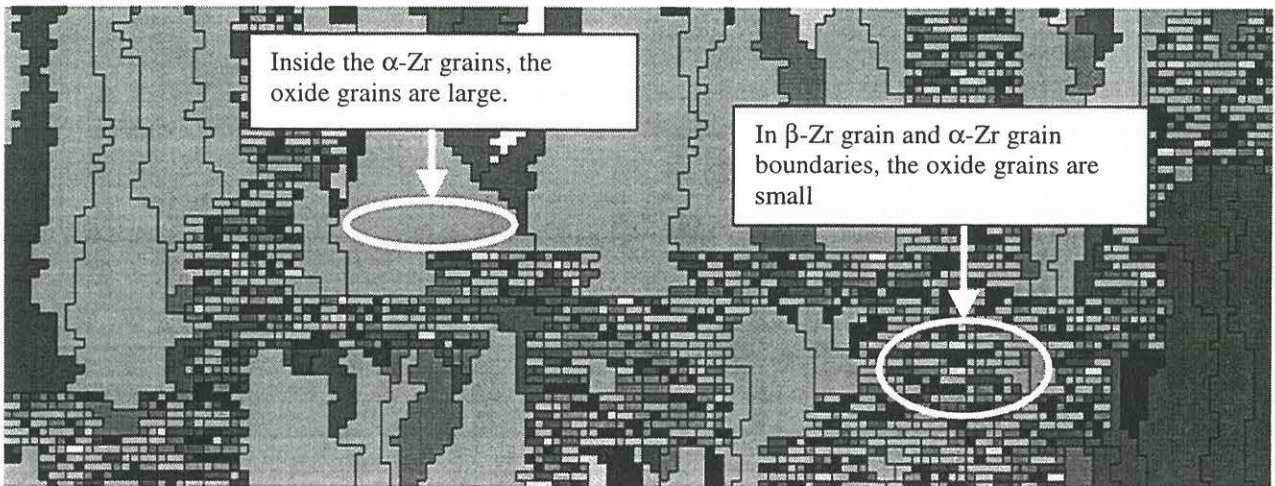


Fig.3 Oxide grain size distribution in different substrate locations

## VERIFICATION OF THE MODEL

In order to verify this model, we simulated the oxide texture formation on various Zr substrates. The understanding of oxide texture is the signature of the understanding of oxidation process, and accurate prediction of texture development may be considered as a proof of the correctness of the simulation. In monoclinic crystal system, there are total as many as 26011 orientations if the orientation space is defined within 5 degree angular interval. If the model can predict  $ZrO_2$  oxide orientation distribution, we believe somehow the model is correct. We have used this model to simulate the oxide texture development on Zr-2.5Nb specimens cut from fuel channel Zr-Nb tube along three different planes perpendicular to radial, transverse and longitudinal

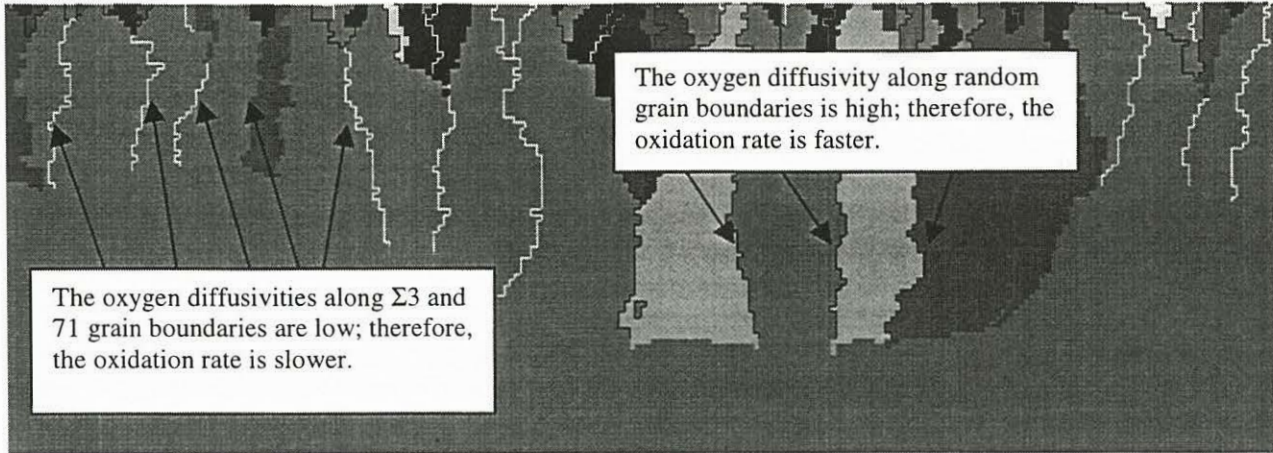


Fig. 4 Oxide grain boundary character distribution

directions, and also Zircalloy – 4 specimens. The results of simulation<sup>2-5, 13, 14</sup> are in good agreement with experiments. For example, figure 5 shows the comparison of the inverse pole pole figures obtained from the simulation and experiment for Zr-2.5Nb (RD cuttings). Both inverse pole figures indicate that the [10-6] axes of oxide grains are parallel to the sample normal direction. In monoclinic system, [10-6] is the normal direction of (10-4) crystallographic plane.

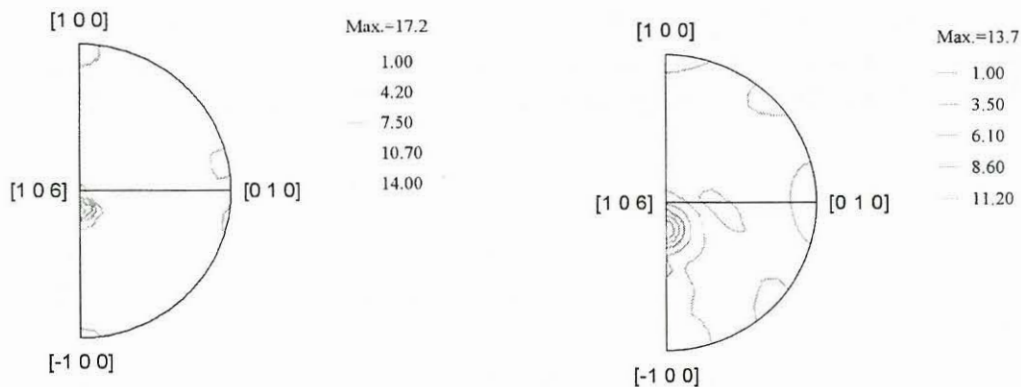


Fig. 5 Simulated (left) and experimental (right) oxide inverse pole figures of on Zr-2.5Nb

## APPLICATIONS

Effects of Oxide Grain Boundaries Character Distribution on Oxidation Kinetics. In Zr-2.5Nb the oxidation kinetics is affected by many factors, such as, a character of the oxide grain boundaries, substrate grain size, substrate orientation and phase composition. To separate the effects of these factors is not easy. Especially, the changes of oxide texture and grain boundary character distribution are often linked and it is difficult to separate a role they play in affecting the oxidation kinetics. In order to overcome this difficulty, in simulation we have designed two

single crystal substrates with different orientations: (11-20)[1-100] and (13-46)[4-511]. The former is the Zr-2.5Nb tube radial direction ideal orientation on which the lattice matching of oxide nuclei and the substrate is likely to occur, and the later is an arbitrary orientation on which the lattice matching between the oxide nuclei and the substrate is more difficult to occur. These orientations represent two extreme cases; in the former case, one expects extremely high percentage of special grain boundaries ( $\Sigma 3$  and 71) and low angle grain boundaries, because the lattice matching is so strong that the oxide orientations are either similar or in some special relationships with each other. In the later case, one expects high amount of high angle grain boundaries because oxide orientations are more random.

As one can see in Fig. 6, the total amount of  $\Sigma 3$ , 71, and low angle grain boundaries is about 50% for (11-20)[1-100] single crystal substrate. On the other hand, the total amount of the same boundaries is less than 5% on (13-46)[4-511] substrate. We also found that the amount of special and low angle grain boundaries increases and the amount of high angle grain boundaries decreases as the oxidation continues in both cases. The oxidation time is represented by MCS(Monte Carlo Steps). In this case, because the substrates are single crystals, the nucleation of oxide takes place only on the substrate surface. When the oxide grains start to grow, they will grow continuously and re-nucleation of oxide will not be observed because of the absence of the nucleation sites, i.e.  $\alpha$ -Zr grain boundaries and  $\beta$ -Zr. According to our original assumptions, during the growth stage, some orientations, namely (10-4), grow faster than others because the minimization of the elastic energy in the oxide film favours this orientation. Thus, the oxide texture becomes stronger and stronger as the oxidation continues. Stronger texture results in a high portion of special and low angle grain boundaries and low portion of high angle grain boundaries.

Since the oxygen diffusivities along  $\Sigma 3$ , 71, and low angle grain boundaries are lower than that along higher angle grain boundaries, the increase in the amount of  $\Sigma 3$ , 71, and low angle grain boundaries will lead to the decrease of the oxidation rate. This is shown in Fig. 7. The difference

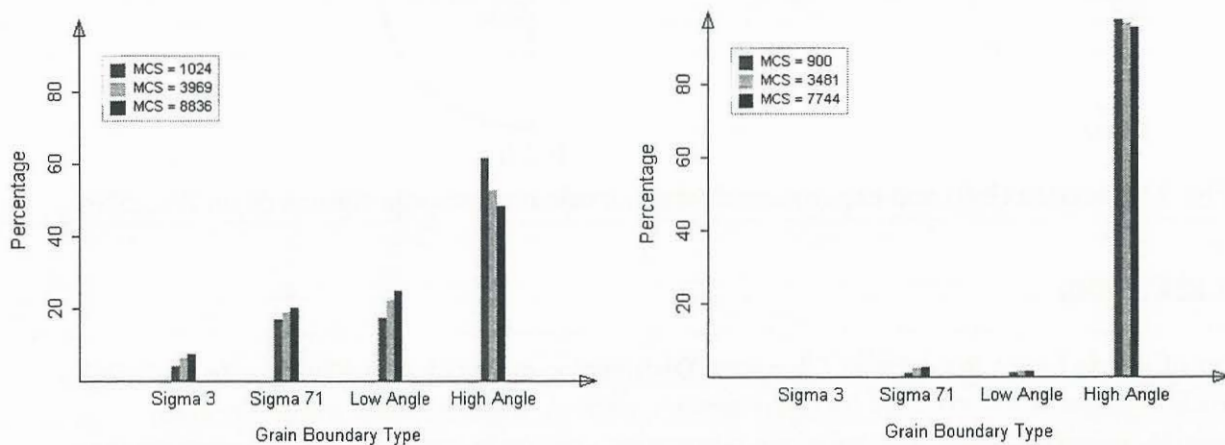


Fig. 6 Grain boundary character distributions of the oxide formed on (11-20)[1-100] (left) and (13-46)[4-511] (right) single crystal substrates.

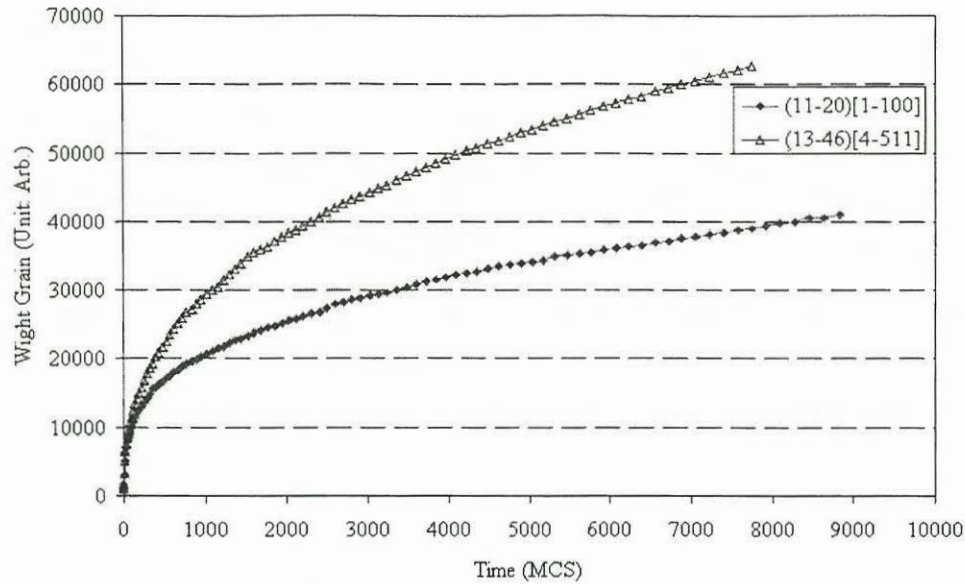


Fig. 7 Oxidation kinetics of (11-20)[1-100] and (13-46)[4-511] single crystal substrates.

of the fitted parabolic rate constants in the two investigated cases is about two times.

Effects of Zr Substrate Microstructure and  $\beta$ -Phase Distribution on Oxidation Kinetics: Three samples (RD, TD and LD) were oxidized at 400°C in air for 12 hours. The samples were cut from Zr-2.5Nb pressure tube with their normal directions parallel to the radial, transverse, and longitudinal directions of the tube respectively as shown in Fig. 8. The experimental and simulated kinetics of the three samples are given in Fig. 9. Both the experimental and simulation results show that the parabolic rate constants of the three samples are approximately in the ratio of 1 : 2 : 2.5.

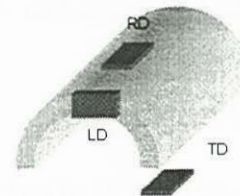


Fig. 8 Sample cuttings

The above difference in oxidation kinetics maybe the consequence of the substrate microstructure changes due to the different sample cuttings. The  $\alpha$ -Zr grain in the pressure tubes has anisotropic shape with an aspect ratio of about 1:5:50 in the radial, transverse and longitudinal direction respectively. The grains are surrounded by a thin network of metastable  $\beta$ -Zr phase<sup>27</sup>. Since the  $\alpha$ -Zr grain is not equiaxial, their grain size and shape, will be different when observed in the samples cut at different directions with respect to the pressure tube axis. As a result the distribution of the  $\alpha$  grain boundaries and  $\beta$  phase grains in the specimen is different for each sample. Since these structural elements are typical nucleation sites, small oxide nuclei are formed at these locations, as one can observe in Fig. 3. Thus, the microstructure generated by the three different cuttings significantly affects the oxide nucleation and microstructure and as well the transport of oxygen through the oxide. Therefore, the oxidation rate is different for RD, TD, and LD samples.

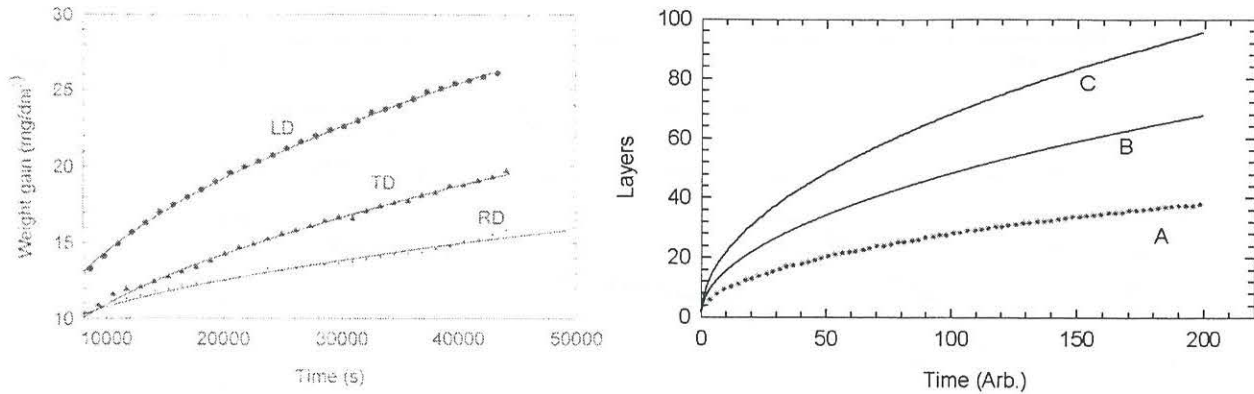


Fig. 9 Experimental (left) and simulated (right) oxidation kinetics

## HYDROGEN INGRESS

This computer model has been developed to understand and predict hydrogen transport through oxide. The nature of hydrogen transportation is more complex and difficult to measure in experiments<sup>29-31</sup>. Our preliminary results show that hydrogen pick-up and oxide film thickness changes strongly correlated to each other. The sample with thicker oxide film always has higher hydrogen pick-up, as show in Fig. 10. This suggested that hydrogen ingress is possibly controlled by a diffusion process similar to oxygen diffusion through oxide. We believe that the oxide grain size shown in Fig. 3 and grain boundary character distribution shown in Fig. 4 and Fig. 6 must play important role in controlling hydrogen diffusion and hydrogen trapping processes.

## CONCLUSIONS

The proposed model of oxidation is incorporated in computer software. The software is a fully automated and mechanism of oxidation can be arbitrarily defined. The software is window based and simulation program has capacity to be modified and extend. It is designed to help research specialists to model Zr oxidation and hydrogen permeation processes and can help to understand and possibly predict hydrogen permeation through complex structure of oxides. It can be used to computer design the pressure tube structure with maximum resistance against hydrogen ingress. At current stage, we can use this software to perform the following tasks:

- † Simulate the effects of substrate texture on oxidation and hydrogen permeation
- † Simulate the effects of substrate grain size on oxidation and hydrogen permeation
- † Simulate the effects of substrate grain shape and grain boundary networks on oxidation and hydrogen permeation
- † Simulate the effects of  $\beta$  phase distribution on oxidation and hydrogen permeation

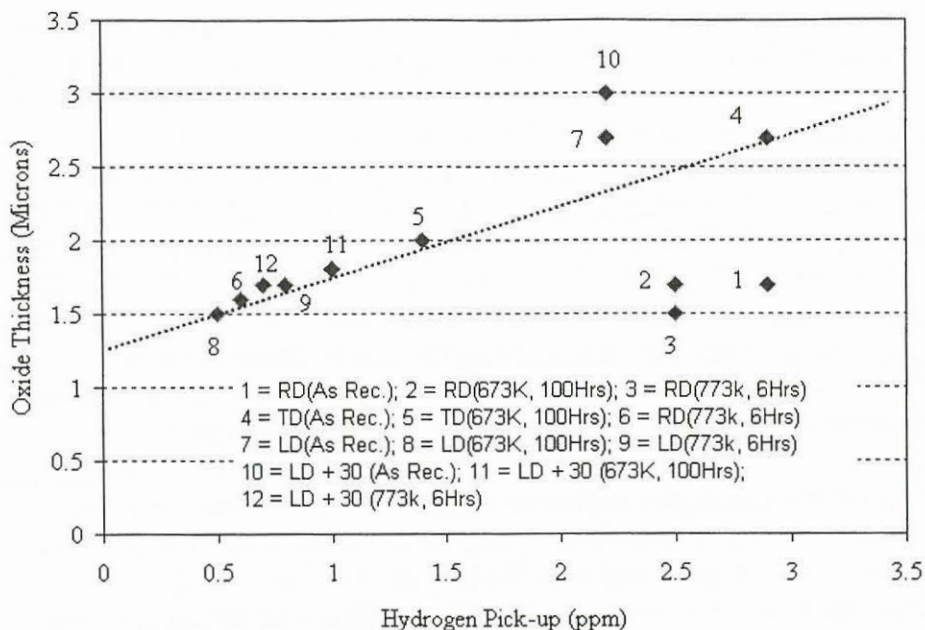


Fig. 10 The relation between oxide thickness and hydrogen pick-up.

- † Design substrate structure to optimize the resistance of Zr tube against hydrogen permeation
- † Simulate oxidation kinetics, hydrogen permeation
- † Simulate oxide texture, grain size distribution, grain boundary character distribution
- † Monitor oxidation and hydrogen permeation processes instantly and graphically

#### REFERENCE:

1. Li, H. and Szpunar, J., "Computer Simulation of Diffusion Process in Polycrystalline Material", "Defect and Diffusion Forum", 194 – 199, p1227 (2001)
2. Li, H., "Computer Simulation of Oxide Texture and Microstructure Formation and their Effects on Oxidation Kinetics", Ph.D. Thesis, McGill University (1999)
3. Li, H., Glavicic, M. and Szpunar, J., "Simulation of Texture Formation in ZrO<sub>2</sub> Film Grown on Zr-2.5%Nb", Textures and Microstructures 34, pp. 75-90 (2000)
4. Li, H., and Szpunar, J., "Computer Simulation of the Diffusion Activation Energy in ZrO<sub>2</sub> Grain Boundary", Third International Conference on Grain Growth, Pittsburgh PA, Proceedings of the Third International Conference on Grain Growth, TMS publication, Edited by H. Weiland, B.L. Adams and A.D. Rollett, pp. 339-343 (1998)
5. Li, H., Glavicic, M. and Szpunar, J., "A Model of Texture Formation in ZrO<sub>2</sub> Films", Materials Science and Engineering A, accepted (2002)
6. Glavicic, M., and Szpunar, J., "Phase Analysis and Grazing Incidence Stress Measurement in ZrO<sub>2</sub> Films", Proceedings of the Twelfth International Conference in Textures of Materials (ICOTOM-12), Montreal, Canada, NRC Research Press, Edited by J.A. Szpunar, Volume 1, pp. 110-115 (1999)

7. Glavicic, M., Szpunar, J., and Lin, Y., "The Role of Oxide Texture in the Protection of Zr-2.5%Nb Alloy Pressure Tubes Against Hydrogen Ingress", Proceedings of the Twelfth International Conference in Textures of Materials (ICOTOM-12), Montreal, Canada, NRC Research Press, Edited by J.A. Szpunar, Volume 2, pp. 1409-1414 (1999)
8. Gertsman, V., Lin, Y., Zhilyaev, A., and Szpunar, J., "Special Grain Boundaries in Zirconia Corrosion Films", Philosophical Magazine A, Vol. 79, No. 7, pp. 1567-1590 (1999)
9. Zhilyaev, A., and Szpunar, J., "Influence of Growth Stress on Oxidation Kinetics in Oxide Film Formed on Zirconium Alloy Tubes", J of Nuclear Mat. 264, pp. 327-332 (1999)
10. Zhilyaev, A., and Szpunar, J., "Stress-Induced Diffusion and Breakdown in Thin Films of Nanocrystalline Zirconia", Third International Conference on Grain Growth, Pittsburgh PA, Proceedings of the Third International Conference on Grain Growth, TMS publication, Edited by H. Weiland, B.L. Adams and A.D. Rollett, pp. 549-556 (1998)
11. Zhilyaev, A., Gertsman, V., and Szpunar, J., "Self-Organized Clusters of Microstructure in Zirconia Film", Third International Conference on Grain Growth, Pittsburgh PA, Proceedings of the Third International Conference on Grain Growth, TMS publication, Edited by H. Weiland, B.L. Adams and A.D. Rollett, pp. 715-720 (1998)
12. Zhilyaev, A., Szpunar, J., and Gertsman, V., "Statistical Characterization of Grain Boundaries in Nanocrystalline Zirconia", Nanostructured Materials, 9,1-8, pp. 343-346 (1997)
13. Lin, J. and Szpunar, J. A., "Examination of the Stress and Phase Composition in Textured Zirconium Oxides Films", Proceeding of 12th International Conference on Textures of Materials, vol. 2, pp. 1439-1444 (2002)
14. Lin, J., Cao, X., and Szpunar, J. A., "The Influence of Texture and Microstructure of Zr-2.5Nb Substrate on the Oxidation Kinetics", Journal of Materials Science Forum (Special Volume), p. 1013 (2002)
15. Lin, Y. P., Woo, O. T. and Lockwood, D.J., Polycrystalline Thin Films: Structure, Properties and Applications, MRS Symp. Proc., 343, p. 487 (1994)
16. Cox, B. and Pemsler, J. P., J. Nucl. Mater., 28, p.73 (1968)
17. Cox, B. and Roy, R., Journal of Electrochemical Technology, 4, p 121 (1966)
18. Roy, C. and David, G., J. Nucl. Mater., 37, p. 71 (1970)
19. Baily, J. E., J. Nucl. Mater, 8, p. 259 (1963)
20. Baily, J. E., Proc. 3<sup>rd</sup> Eur. Reg. Cong. Om E.M., A-395, (1964)
21. Ploc, R. A., J. Nucl. Mater., 113, p. 75 (1983)
22. Ploc, R. A., J. Nucl. Mater. 110, p. 59 (1982)
23. Ploc, R. A., J. Nucl. Mater. 113, p. 75 (1983a)
24. Ploc, R. A., J. Nucl. Mater. 115, p. 110 (1983b)
25. Ploc, R. A., J. Nucl. Mater. 28, p. 48 (1968)
26. Sabol, G.P. and McGonald, S. G., "Stress Effects and the Oxidation of Metals", p. 352 (1975)
27. Urbanic, V. F., Chan, P. K., Khatamian, D., and Woo, O.-T.T., Zirconium in the Nuclear Industry, Tenth International Symposium, p. 116 (1994)
28. Godlewski, J., Zirconium in the Nuclear Industry: Tenth International Symposium, p. 663 (1994)
29. Khatamian, D., Journal of Alloys and Compounds, 253-254, p. 471 (1997)
30. Stern, A., Khatamian, D., Laursen, T., Weatherly, G. C., and Perz, J. M., Journal of Nuclear Material, 148, p. 257 (1987)
31. Aitchison, I., Khatamian, D., and Hartog, J., Zeitschrift fur Physikalische Chemie, 181, p. 1005 (1993)